Development of a Micromanipulation System with Force Sensing

Shahzad Khan, Ahmet Ozcan Nergiz, Asif Sabanovic and Volkan Patoglu

***Abstract*— This article provides in-depth knowledge about our undergoing effort to develop an open architecture micromanipulation system with force sensing capabilities. The major requirement to perform any micromanipulation task effectively is to ensure the controlled motion of actuators within nanometer accuracy with low overshoot even under the influence of disturbances. Moreover, to achieve high dexterity in manipulation, control of the interaction forces is required. In micromanipulation, control of interaction forces necessitates force sensing in nano-Newton range. In this paper, we present a position controller based on a discrete time sliding mode control architecture along with a disturbance observer. Experimental verifications for this controller are demonstrated for 100, 50 and 10 nanometer step inputs applied to PZT stages. Our results indicate that position tracking accuracies up to 10 nanometers, without any overshoot and low steady state error are achievable. Furthermore, the paper includes experimental verification of force sensing within nano-Newton resolution using a piezoresistive cantilever end-effector. Experimental results are compared to the theoretical estimates of the change in attractive forces as a function of decreasing distance and of the pull off force between a silicon tip and a glass surface, respectively. Good agreement among the experimental data and the theoretical estimates has been demonstrated.**

I. INTRODUCTION

The major goal of micromanipulation is to design and build functional structures in micro scale using components whose sizes range in the order of microns. Generally, in these scales the laws of Newtonian mechanics are still valid while atomic level effects may also come in play. Thus the scale considered is at the boundary of two traditional spaces whose limits are not well defined [1]–[4]. Since the surface to volume ratio increases inversely proportional to the length scaling factor, at these scales surface properties and forces start to dominate bulk properties of micro particles, a fact mainly called as scaling effect [5]. As a result, the dynamics of micro-particles are mainly dominated by friction and stiction forces as well as attractive or repulsive particle level forces (van der Waals, Casimir, capillary, hydrogen bonding, ... etc.) that act through long or short range effects.

Manipulating objects with higher dexterity requires not only precise positioning of actuators with nanometer accuracy but also control and compensation of forces involved in the manipulation process. Micromanipulation with force control is an emerging area that appears certain to eventually become an important component in microsystems technology.

Mechatronics Engineering Programme, Faculty of Engineering and Natural Sciences, Sabanci University, 34956, Istanbul, Turkey. {shahzad, ahmetn}@su.sabanciuniv.edu {asif, vpatoglu}@sabanciuniv.edu

Much of the research effort for micromanipulation in the past has been directed to using piezoelectric stack (PZT) actuators as nano positioners due to unique characteristics, such as high resolution in nanometer range, high position bandwidth up to several kilo hertz, large force output up to few tons and appropriate working stroke within millimeter range [6]. However, PZTs suffer from nonlinearities between the input (voltage) and the output (position). The major portion of nonlinearities arise due to the parasitic hysteresis characteristics of the piezoelectric crystal while other nonlinear effects are results of internal disturbances from creep and thermal drift. Many attempts have been done to model hysteresis and incorporate this model into the control loop to eliminate aforementioned detrimental effects of hysteresis helping to ensure nano-meter level positioning accuracies [7]–[9].

Since manipulating an object requires not only the ability to observe and position, but also to physically interact with the object, micro manipulators solely based on visual feedback and position control [10], [11] are not effective for dexterous micromanipulation. For manipulating micro objects, especially delicate structures or biological material, pure position control is not even safe to ensure successful operation. Force control is often needed to augment the operation in order to achieve better manipulation results. Moreover, in certain applications such as individual cell-based diagnosis or pharmaceutical tests, obtaining the interaction force is the main objective. Such applications involve probing or reconstructing the state of objects using the micro/nano scale interaction forces between the manipulator and the sample [12]. For example, the developmental stages of zebrafish eggs can be estimated by examining micro/nano scale forces required to penetrate inside the egg envelope since this interaction force is proportional to the thickness of egg envelope [13].

In the past, many researchers have developed micromanipulation systems [14]–[17]. In this paper, a micromanipulation system with open architecture is presented. The unique features of the system include a discrete time sliding mode controller utilized to drive the PZT stages and a disturbance observer designed to cope up with the parametric changes and unmodeled nonlinearities. The system can achieve nanometer level position accuracy under closed loop position control and is capable of nano-Newton level force sensing using piezoresistive cantilever.

The paper is organized as follows. Section II explains the micromanipulation setup. Section III describes the model of the piezostages used in model based controller. In Section IV, the derivation of the discrete time sliding mode controller

along with the disturbance observer is undertaken. Section V demonstrates the experimental validation of position control of PZT stages while Section VI shows the experimental validation of force sensing. Finally, Section VII concludes the paper and discusses future directions.

II. MICROMANIPULATION SETUP

In order to develop adequate systems for efficient and reliable manipulation of objects at micro scale, it is necessary to have position control with nanometer accuracy and force sensing/estimation in nano-Newton scales. Moreover, for visual feedback of the process high magnification microscopy is essential. In order to fulfill the above requirements, we have developed an open architecture micromanipulation system as shown in Figure 1.

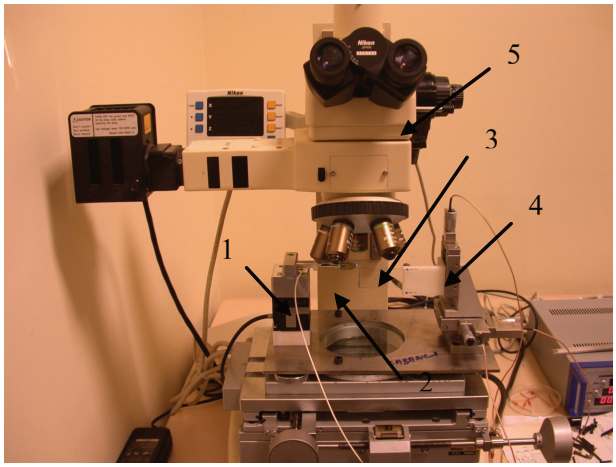

Fig. 1. Experimental micromanipulation setup: 1-Closed loop PZT stages, 2-Piezoresistive cantilever, 3-Glass slide, 4-Open loop PZT stages, 5-Microscope

Three axes piezo stages (P-611 by Physik Instrumente) are utilized for nano scale positioning of a microcantilever. The piezo stages are driven by a power amplifier (E-664) in closed loop external control mode. Position of the closed loop stages are measured by potentiometers (strain gauge sensors) integrated in the amplifier. The piezo stages possess a travel range 100 micrometer per axis with a theoretical resolution of one nanometer. The stages are equipped with compliant guiding systems, which have zero stiction and friction. As the base stage, an open loop piezoelectric micrometer drive (PiezoMike PI-854 from Physik Instrumente) has been utilized [18]. The base stage is equipped with integrated high resolution piezo linear drives. The linear drives can be operated manually with a resolution of 1 micrometer. By controlling the piezo voltage, the micrometer tip can be automatically moved in and out up to 25 micrometers with respect to the manually set position. The resolution of piezoelectric motion is in the sub-nanometer range. The piezoelectric actuators are driven by a low voltage piezo driver (E-663) in external control mode. As a control platform DS1103 from dSpace is utilized. A flexible programming environment has been developed in C that can easily accommodate any possible hardware changes.

For visual feedback, a Nikon MM-40 optical microscope is utilized. The magnification of the microscope ranges from 10x to 100x with a working distance of $75\,mm$ to $0.32\,mm$, respectively.

Force sensing is achieved through a piezoresistive microcantilever (from Applied NanoStructures) made out of silicon. The microcantilever is $300\,\mu m$ in length, $50\,\mu m$ in width and $1.6\,\mu m$ in thickness. The piezoresistive microcantilever has a base resistance of $1.2\,k\Omega$ and the resistance values varies from $900\,\Omega$ to $2\,k\Omega$. A $25\,\Omega$ resistance change corresponds to a cantilever deflection $5\,\mu m$. The sensitivity of cantilever is rated at $5 \times 10^{-5}\,\Omega/A^{\circ}$.

III. MODELING THE PIEZO-STAGE

Since the PZT stages are made out of piezoceramic, a well studied dielectric material, one would expect PZT stack actuators to inherit their properties and to exhibit capacitive behavior along with rate-dependent hysteresis. The hysteresis is a parasitic affect which affects the net electrical charge delivered to the actuator. Additionally, the endpoint displacement of the stages as a function of electrical charge can be accurately modeled using a second-order lumped linear dynamic model.

In this paper, a fairly accurate approximate model for the piezo stage is chosen from [7] due to its ease of implementation and accuracy at estimating the actual behavior of these actuators. The piezo stages consist of a piezo drive with a flexure guided structure which is designed to possess zero stiction and friction. Moreover, the flexure stages exhibit high stiffness, high load capacity and are insensitive to shock and vibration. Figure 2 depicts the overall electromechanical model of a PZT actuator [7].

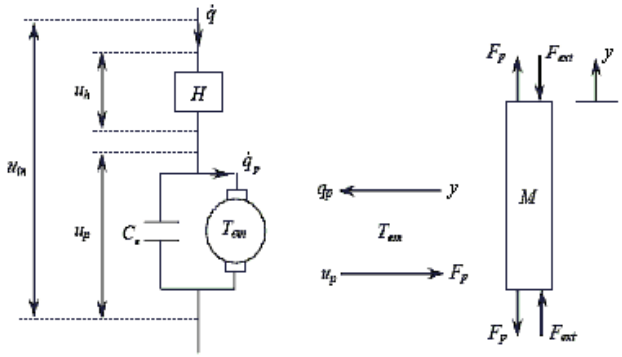

Fig. 2. Electromechanical model of a PZT actuator

In the model adapted from [7] the hysteresis and piezoelectric effects are separated and modeled in a serial fashion. In the model, the symbol H represents the hysteresis effect and u_h corresponds to the voltage as a result of this effect. The piezoelectric effect is modeled as an ideal electromechanical transducer with transformer ratio of T_{em}. The capacitance C_e represents the lumped capacitance of the individual PZT

wafers, which are electrically in parallel. The total current flowing through the circuit is given by $\dot{q}$, where q is defined as the total charge in the PZT actuator. The charge q_p denotes the transducer charge from the mechanical side whereas the voltage u_p is due to the piezo effect. The total voltage over the PZT actuator is u_{in}. The force F_p is the transducer force from the electrical side, while F_{ext} is the externally applied force. The elongation of the PZT actuator is denoted by y. The mechanical relationship between F_p and y is defined as M. Note that, as a result of ideal transformer assumption the electrical and mechanical energy at the ports of interaction are equal: $u_p q_p = F_p y$.

The modulus of elasticity, viscosity, and mass density of the piezoelectric ceramic are denoted by E, ν, and ρ, respectively. The PZT actuator have a length of L and a cross-sectional area of A. Effective mass m_p, stiffness k_p and damping coefficients c_p can be calculated as

$$m_p = \rho A_p L \quad (1)$$

$$k_p = \frac{\rho A_p}{L} \quad (2)$$

$$c_p = \frac{\nu A_p}{L}. \quad (3)$$

Finally, the coupled equations governing the electromechanical behavior of the piezo stages can be written as

$$m_p \ddot{y} + c_p \dot{y} + k_p y = T_{em}\left(u_{in}(t) - H(y, u_{in})\right) - F_{ext}. \quad (4)$$

where y represents the displacement of the piezo stage and H denotes the non-linear hysteresis which is a function of y and u_{in}. There exists several hysteresis models to literature [7]–[9], [18]; however, due to dependence of these models in many factors, model based compensation of hysteresis is a cumbersome process. In the following section, a disturbance observer is proposed to compensate for hysteretic effects in the system.

IV. DESIGN OF DISCRETE TIME SLIDING MODE CONTROLLER AND DISTURBANCE OBSERVER

To derive the controller structure, Eqn. (4) governing the behavior of the piezo stages can be rewritten in state-space form as

$$\dot{x}_1 = x_2 \quad (5)$$

$$\dot{x}_2 = -\frac{k_p}{m_p}x_1 - \frac{c_p}{m_p}x_2 + \frac{T_{em}}{m_p}u_{in} - \frac{T_{em}}{m_p}H - \frac{F_{ext}}{m_p} \quad (6)$$

or in a more general form as

$$\dot{x} = f(x, H, F_{ext}) + B u_{in}. \quad (7)$$

The aim of the controller is to drive the states of this system into the set S defined by

$$S = \{x : G(x^r - x) = \sigma(x^r, x) = 0\}. \quad (8)$$

where $G = [\lambda \ 1]$ with λ being a positive constant, $x = [x_1 \ x_2]^T$ is the state vector, $x^r = [x_1 \ x_2]^T$ is the reference vector, and $\sigma(x^r, x)$ is the function defining the sliding mode manifold.

With a proper selection of control Lyapunov function $V(\sigma)$, to ensure the stability of the system the Lyapunov function derivative $\dot{V}(\sigma)$ leads to the function

$$\sigma(\dot{\sigma} + D\sigma) = 0 \quad (9)$$

where D is a positive constant. A solution for Eqn. (9) is given by

$$(\dot{\sigma} + D\sigma) = 0. \quad (10)$$

Substituting in the derivative of the sliding surface into this equation, one can derive

$$\dot{\sigma} = G\dot{x}^r - Gf - GBu(t) = GB(u_{eq} - u(t)) \quad (11)$$

where $u_{eq} = \frac{\dot{x}^r - f}{B}$. Solving for $u(t)$, the control input can be calculated as

$$u(t) = u_{eq} + (GB)^{-1} D\sigma. \quad (12)$$

However, in this formulation the equivalent control as given in Eqn. (12) is difficult to calculate. To achieve a controller form that is more suitable for digital implementation, one can discretize Eqn. (12) using the forward Euler's method. Solving for the equivalent control after discretization, one can derive

$$u_{eq}(kT_s) = u(kT_s) + (GB)^{-1}\left(\frac{\sigma((k+1)T_s) - \sigma(kT_s)}{T_s}\right) \quad (13)$$

However, Eqn. (13) is not casual. A casual form of this equation can be derived by approximating the current value of the equivalent control with a single-step backward value estimated from Eqn. (13)

$$\hat{u}_{eq_k} = u_{eq_{k-1}} = u_{k-1} + (GB)^{-1}\left(\frac{\sigma_k - \sigma_{k-1}}{T_s}\right). \quad (14)$$

where $\hat{u}_{eq}$ (or $\hat{u}_{eq}(kT_s)$) is the estimate of the current value of the equivalent control. Inserting Eqn. (14) into Eqn. (13) the control structure can be finalized as

$$u_k = u_{k-1} + (GBT_s)^{-1}\left((DT_s + 1)\sigma_k - \sigma_{k-1}\right). \quad (15)$$

The observer structure is deduced based on the Eqn. (4) under the assumption that all the plant parameters uncertainties, nonlinearities and external disturbances can be represented as a lumped disturbance. It is assumed that y is the measurable displacement and $u(t)$ is the input, which is also a measurable quantity.

$$m_p \ddot{y} + c_p \dot{y} + k_p y = T_p u(t) - F_{dist} \quad (16)$$

In this equation, $F_{dist} = T_p H + \Delta T(v_{in} + v_h) + \Delta m\ddot{y} + \Delta c\dot{y} + \Delta k y$, where m_p, c_p, k_p and T_p are the nominal plant parameters while Δm, Δc, Δk and ΔT are the uncertainties associated with the plant parameters. Since y and $u(t)$ are measurable, the observer structure can be written in following form:

$$m_p\ddot{\hat{y}} + c_p\dot{\hat{y}} + k_p\hat{y} = T_p u - T_p u_c. \tag{17}$$

In the observer equation $\hat{y}$, $\dot{\hat{y}}$, and $\ddot{\hat{y}}$ are the estimated position, velocity, and acceleration, respectively. The plant control input is denoted by u whereas u_c is the observer control input.

If estimated position $\hat{y}$ is to be forced to track y, then a sliding surface σ_{obs} can be written in the same structure as done for the controller derivation above

$$\sigma_{obs} = \lambda_{obs}(y - \hat{y}) + (\dot{y} - \dot{\hat{y}}). \tag{18}$$

Following similar steps as done for the sliding mode controller derivation above, the model of the observer can be easily derived as

$$u_{c_k} = u_{c_{k-1}} - \frac{m_p}{T_p}\left(D_{obs}\lambda_o bs + \frac{\sigma_{obs_k} - \sigma_{obs_{k-1}}}{T_s}\right) \tag{19}$$

The control structure in Eqn. (15) along with the disturbance observer structure in Eqn. (19) is suitable for implementation. Thus a discrete time sliding mode controller along with a disturbance observer is utilized for piezo actuation as shown in Figure 3.

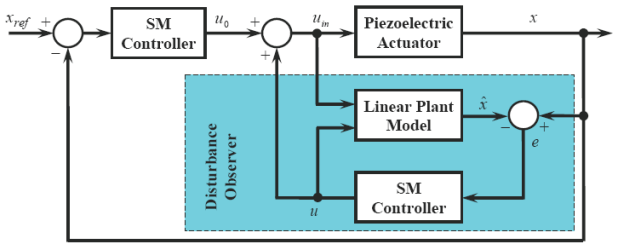

Fig. 3. Overall controller structure

V. EXPERIMENTAL VALIDATION OF POSITION CONTROL

In order to verify the performance of discrete time sliding mode controller along with the disturbance observer, smooth step inputs are given to one of the piezo stages and responses are drawn in Figure 4.

As it can be observed from Figure 4, the responses for closed-loop performance of 100 nanometers, 50 nanometers and 10 nanometers, respectively, are able to achieve the desired reference position. The rise times and steady state errors are 30 ms, 23 ms, and 22.5 ms; and 1%, 2%, and 8%, for 100, 50 and 10 nanometers, respectively. In none of these tested cases an overshoot behavior is observed.

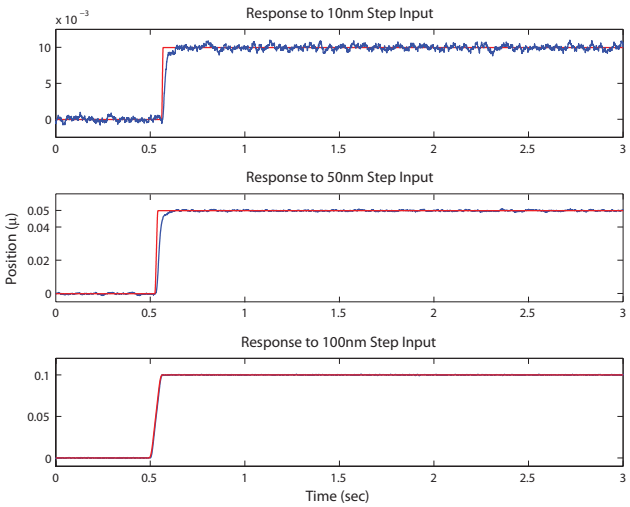

Fig. 4. Experimental setup for micromanipulation, 1-Nanocube, 2-Piezoresistive cantilever, 3-Glass slide, 4-Open loop PZT, 5-Nikon MM-40 Microscope

Operation with no overshoot is the foremost requirement for micromanipulation applications. From these experiments we can conclude that the proposed controller along with the disturbance observer produces acceptable results. However, the system suffers from noise coming from the measurement devices, which shows up in the steady state plots of the system.

VI. EXPERIMENTAL VALIDATION OF FORCE SENSING

A piezoresistive microcantilever with an integrated lightly-doped strain gauge is utilized as the force sensor. As the force is applied at the free end of the cantilever, the change of resistance takes place depending on deflection. The amount of deflection is measured by a Wheatstone bridge which provides a voltage output, which is amplified by the amplifier as shown in the Figure 5. To match with the initial cantilever resistance value, one of the active resistors in the full bridge is replaced by a potentiometer. The amplified voltage is send to the data acquisition card, and the force is calculated using Hooke's law

$$F = K_c\, z \tag{20}$$

where K_c is the known spring constant of $0.3603 N/m$ and z is the amount of cantilever deflection. The spring constant is calculated by considering a linear beam equation and verified via a natural frequency test using an AFM. The cantilever is mounted on the three axes closed loop stage and the x-axis is moved so that cantilever tip comes in contact with the glass slide which is supported by three axes open loop PZT actuators. The interaction (contact and non-contact) forces between the tip and glass slide are measured. The force measurement data is shown in Figure 5. The movement of the cantilever is selected to be perpendicular to the plane of the optical axis in order to achieve better visibility of the

distance between the cantilever and the glass slide. Since the displacement range of the x-axis of the closed loop stage is $100\,\mu m$, the glass slide is brought within the range using open-loop manual PZT axes. Finally. the change of the resistance is converted to change in voltage (millivolt range) using the full bridge, which in turn is converted to $\mp 10\,V$ range using the amplifier.

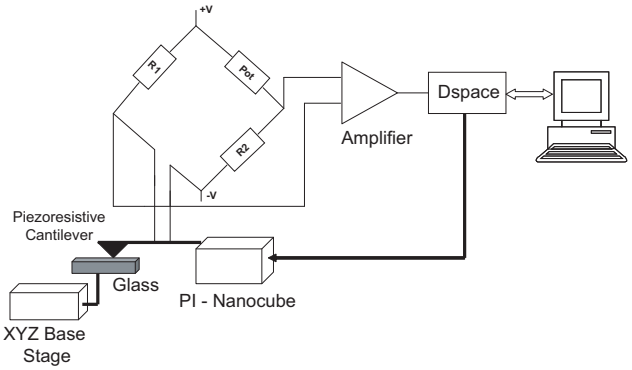

Fig. 5. Force measurement setup

Figure 6 presents the attractive forces for a smooth step between the tip and glass slide. As the distance between the tip and glass slide decreases the attractive forces increases. The first part of the graph is dominated by electrostatic forces while the remaining part is dominated by van der Waals forces. The change in slope of the force measurement plot corresponding to these two regions can be observed from Figure 6.

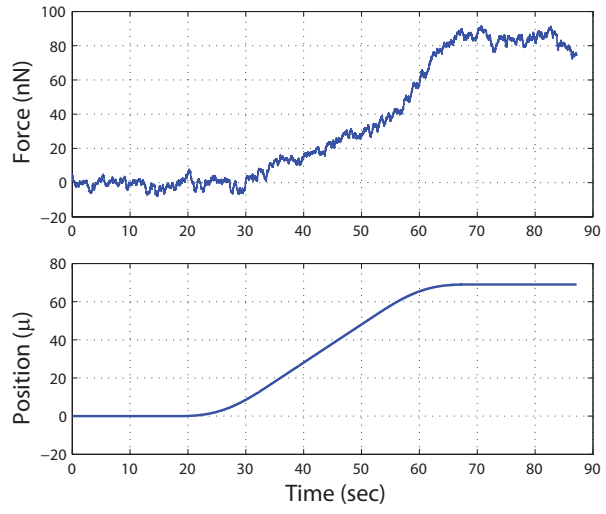

Fig. 6. Force Response for Smooth Step Position References

In order to verify force measurement, theoretical values of pull-off force (breaking load during the withdrawal of tip) between the silicon tip and the glass surface is compared with the experimental results. In case of the interaction between a spherical tip and a planar surface, the interaction force can be approximated by Dugdale model [19], [20] as

$$F_{pull-off} = \left(\frac{7}{4} - \frac{1}{4}\frac{4.04\lambda^{\frac{1}{4}} - 1}{4.04\lambda^{\frac{1}{4}} + 1}\right)\pi W R \qquad (21)$$

where W is the work of adhesion between the two mediums, R is the radius of the sphere and λ is a coefficient, which can be used to choose the most appropriate contact model for a give case [21]. Using the interfacial energy [22], the pull-off force can be calculated for $\lambda = 0.54$ according to the Dugdale model as $39.43\,nN$ [14]. Figure 7 demonstrates experimentally determined the pull-off force is close to $40\,nN$.

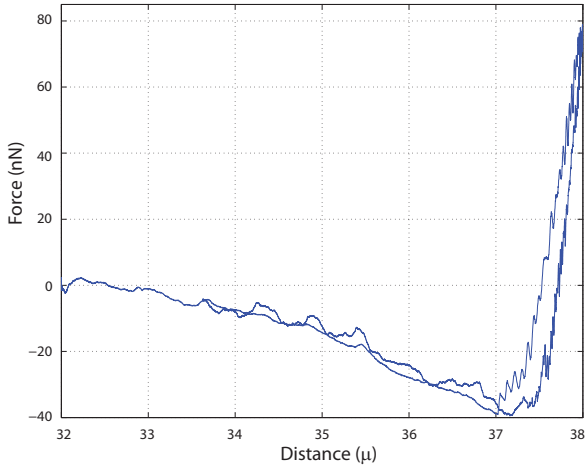

Fig. 7. Force curve for interaction between a silicon tip and a glass surface.

VII. CONCLUSIONS AND FUTURE WORKS

In this article, an ongoing development effort to build an experimental setup of micromanipulation workstation with force sensing using piezoresistive microcantilever is presented. Design of a discrete time sliding mode controller based on Lyapunov theory is presented. Linear model of a piezo stage is used with nominal parameters and a disturbance observer is used to compensate the disturbances acting on the system in order to achieve nano scale positioning accuracies. The effectiveness of the controller and disturbance observer is demonstrated in terms of closed loop position performance. Piezoresistive cantilever is utilized along with a full bridge in order to achieve the nano-Newton level interaction forces between piezoresistive probe tip and a glass surface. Experimental results are compared to the theoretical estimates of the change in attractive forces as a function of decreasing distance and of the pull off force between a silicon tip and a glass surface, respectively. Good agreement among the experimental data and the theoretical estimates has been demonstrated.

As a part of future work, our effort will be directed towards achieving force control for micromanipulation applications. A teleoperated micromanipulation architecture under bilateral control is also planned.

VIII. ACKNOWLEDGMENTS

The authors gratefully acknowledge the financial contributions by TUBITAK, Ankara and Yousef Jameel Scholarship, Berlin.

REFERENCES

[1] R. P. Feyman, "There is plenty of room at the bottom," in *Annual meeting of the American Physical Society*, 1959.

[2] R. S. Fearing, "Survey of sticking effects for microhandling," in *IEEE/RSJ Intelligent Robots System*, pp. 212–217, 1995.

[3] Y. Rollot, S. Regnier, and J.-C. Guinot, "Micro-robotics. a dynamical model of micromanipulation by adhesion.," in *12th CISM-IFToMM symposium. Theory and Practice of robots and manipulator*, pp. 111–118, 1998.

[4] D. S. Haliyo and S. Regnier, "Manipulation of micro-objects using adhesion forces and dynamical effects," in *ICRA/IEEE International Conference of Robotics and Automation.*, 2002.

[5] J. Israelachvili, *Intermolecular and Surface Forces*. ACADEMIC Press, 1991.

[6] B. Zhang and Z. Zhu, "Developing a linear piezomotor with nanometer resolution and high stiffness,," in *IEEE/ASME Transactions on Mechatronics*, vol. 2 of *1*, pp. 22–29, 1997.

[7] M. Goldfarb and N. Celanovic, "Modeling piezoelectric stack actuators for control of micromanipulation," in *IEEE Control Systems Magazine*, vol. 17, pp. 69–79, 1997.

[8] R. Banning, W. L. de Koning, and J. M. T. A. Adriaens, "Modeling piezoelectric actuators," in *IEEE/ASME Transactions on Mechatronics*, vol. 5 of *4*, pp. 331–341, 2000.

[9] S. Khan, M. Elitas, E. D. Kunt, and A. Sabanovic, "Discrete sliding mode control of piezo actuator in nano-scale range," in *IIEEE/ICIT International Conference on Industrial Technology*, 2006.

[10] D. H. Kim, Y. Kim, K. Y. Kim, , and S. M. Cha, "Dexterous teleoperation for micro parts handling based on haptic/visual interface," in *IEEE International Symposium in Micromechatronics*, pp. 211–217, 2001.

[11] Y. Sun and B. J. Nelson, "Microrobotic cell injection," in *IEEE Int. Conference Robot Autotomation*, vol. 1, pp. 620–625, 2001.

[12] Y. Sun, S. N. Fry, D. P. Potasek, D. J. Bell, and B. J. Nelson, "Characterizing fruit fly behavior using a microforce sensor with a new comb-drive configuration," in *Journal of Microelectromechanical System*, vol. 14, pp. 4–11, 2005.

[13] D. H. Kim, Y. Sun, S. Sun, S. H. Lee, and B. Kim, "Investigating chorion softening of zebrafish embryos with a microrobotic force sensing system," in *Journal of Biomechanics*, vol. 38 of *6*, pp. 1359–1363, 2005.

[14] P. Rougeot, S. Regnier, and N.Chaillet, "Force analysis for micromanipulation," in *IEEE CIRA*, pp. 105–110, 2005.

[15] T. Fakuda and F. Arai, "Prototyping design and automation of micro/nano manipulation system," in *IEEE CIRA*, vol. 1, pp. 192–197, 2000.

[16] M. Weck and C. Peschke, "Assembling hybrid microsystems - challenges and solutions.," in *International Precision Assembly Seminar*, 2003.

[17] M. Bengel, T. Gaugel, and D. Malthan, "Building a mini-assembly system from a technology construction kit," in *International Precision Assembly Seminar*, 2003.

[18] S. Khan, A. O. Nergiz, A. Sabanovic, and V. Patoglu, "Hysteresis compensation for open loop piezoelectric linear drives.," in *TOK, Turkish Automatic Control*, 2007.

[19] K. L. Johnson, *A continum mechanics model of adhesion and friction in a single asperity contact:In Micro-nanotribology and its applications*. Kluwer Academic Publishers, 1997.

[20] B. V. Derjaguin, V. M. Muller, and Y. U. P. Toporov, "Effect of contact deformations on the adhesion of particles," in *Journal of Colloid and interface science*, vol. 53 of *2*, pp. 314–326, 1975.

[21] D. Maugis, "Adhesion of spheres : the jkr-dmt transition model using a dugdale model," in *Journal of Colloid and Interface Science*, vol. 150, pp. 243–269, 1992.

[22] M. Sitti and R. Fearing, "Synthetic gecko foot-hair micro-nanostructures as dry adhesives," in *Journal of Adhesion Science Technology*, vol. 17 of *8*, pp. 1055–1073, 2003.